ETH
Eidgenössische Technische Hochschule Zürich
Swiss Federal Institute of Technology Zurich

Seminar for Applied Mathematics SAM

# Detecting Near Resonances in Acoustic Scattering

L. Grubisic and R. Hiptmair and D. Renner

Research Report No. 2022-38
September 2022

Seminar für Angewandte Mathematik
Eidgenössische Technische Hochschule
CH-8092 Zürich
Switzerland

# DETECTING NEAR RESONANCES IN ACOUSTIC SCATTERING

LUKA GRUBIŠIĆ, RALF HIPTMAIR AND DIEGO RENNER

Abstract. We propose and study a method for finding quasi-resonances for a linear acoustic transmission problem in frequency domain. Starting from an equivalent boundary-integral equation we perform Galerkin boundary element discretization and look for the minima of the smallest singular value of the resulting matrix as a function of the wave number $k$. We develop error estimates for the impact of Galerkin discretization on singular values and devise a heuristic adaptive algorithm for finding the minima in prescribed $k$-intervals. Our method exclusively relies on the solution of eigenvalue problems for real $k$, in contrast to alternative approaches that rely on extension to the complex plane.

**Keywords.** Acoustic scattering, quasi-resonances, boundary integral equations, boundary element method, singular values, Wielandt matrix, zero finding

**MSC2020.** 35J05, 65N38, 65F15

## 1. Introduction

1.1. **Acoustic scattering transmission problem.** We consider the scattering of time-harmonic acoustic waves with fixed wave number $k > 0$ at a bounded penetrable homogeneous object with linear material characteristics and occupying the bounded Lipschitz domain $\Omega_i$ in $d$-dimensional Euclidean space, $d = 2, 3$. Modeling in frequency domain leads to the Helmholtz equation [13, Chapter 2]

$$\Delta u + k^2 n(\boldsymbol{x}) u = 0 \quad \text{in} \quad \mathbb{R}^d \tag{1}$$

for the complex amplitude $u = u(\boldsymbol{x}) : \mathbb{R}^d \to \mathbb{C}$ of the total pressure field. In (1) the scattering object is taken into account by the *piecewise constant* spatially varying refractive index $n \in L^\infty(\mathbb{R}^d)$,

$$n(\boldsymbol{x}) = \begin{cases} n_i & \text{for} \quad \boldsymbol{x} \in \Omega_i \,, \\ n_o := 1 & \text{for} \quad \boldsymbol{x} \in \Omega_o := \mathbb{R}^d \setminus \overline{\Omega}_i \,. \end{cases} \tag{2}$$

with a fixed parameter $n_i \in \mathbb{R}$. In this model with normalized wave speed away from the scattering object the wave number $k > 0$ is linked to the frequency $f$ by $k = 2\pi f$. Throughout we interpret (1) in weak sense and seek solutions $u \in H^1_{\mathrm{loc}}(\mathbb{R}^d)$.

A time-harmonic incident wave is described by its complex amplitude $u_{\mathrm{inc}} \in C^\infty(\mathbb{R}^d)$ and supposed to satisfy $(\Delta + k^2) u_{\mathrm{inc}} = 0$. It is incorporated into the model through the Sommerfeld radiation conditions for the scattered field $u_s := u - u_{\mathrm{inc}}$:

$$\mathbf{grad}\, u_s(\boldsymbol{x}) \cdot \frac{\boldsymbol{x}}{\|\boldsymbol{x}\|} - iku_s(\boldsymbol{x}) = o\left(r^{\frac{1-d}{2}}\right) \quad \text{uniformly for} \quad \|\boldsymbol{x}\| \to \infty \,. \tag{3}$$

**Theorem 1** ([27, Lemma 2.7] and references therein)**.** *When the refractive index $n$ is given by* (2)*, the scattering problem* (1) *&* (3) *admits a unique weak solution $u \in H^1_{\mathrm{loc}}(\mathbb{R}^d)$.*

*Date*: September 1, 2022.

In order to recast the model as a transmission problem across the interface $\Gamma := \partial\Omega_i = \partial\Omega_o$, we write $\boldsymbol{\nu}_* \in L^\infty(\Gamma)^d$, $* = i, o$, for the unit normal vector field at $\Gamma$ pointing into the exterior of $\Omega_*$, and introduce the standard trace operators [32, Section 2.6], $* = i, o$,

$$\text{Dirichlet trace operator:} \qquad \gamma_D^* : H^1_{\mathrm{loc}}(\Omega_*) \to H^{\frac{1}{2}}(\Gamma) , \qquad \gamma_D^* u := u|_\Gamma ,$$

$$\text{Neumann trace operator:} \qquad \gamma_N^* : H^1_{\mathrm{loc}}(\Delta, \Omega_*) \to H^{-\frac{1}{2}}(\Gamma) , \qquad \gamma_N^* u := \mathbf{grad}\, u \cdot \boldsymbol{\nu}_*|_\Gamma .$$

With these notations the total field $u_i := u|_{\Omega_i}$ inside the scatterer and the scattered field $u_s := (u - u_{\mathrm{inc}})|_{\Omega_o}$ outside solve the *transmission problem*

$$\Delta u_i + k^2 n_i u_i = 0 \qquad \text{in } \Omega_i , \tag{4a}$$

$$\Delta u_s + k^2 u_s = 0 \qquad \text{in } \Omega_o , \tag{4b}$$

$$\gamma_D^i u_i = \gamma_D^o u_s + g_D \quad \text{on } \Gamma , \tag{4c}$$

$$-\gamma_N^i u_i = \gamma_N^o u_s + g_N \quad \text{on } \Gamma . \tag{4d}$$

with jump data $g_D := \gamma_D^o u_{\mathrm{inc}} \in H^1(\Gamma)$, $g_N := \gamma_N^o u_{\mathrm{inc}} \in L^2(\Gamma)$.

Theorem 1 asserts unique solvability of (4) for all wave numbers $k \geq 0$. This means that true resonances do not exist. More precisely, the solution operator $\mathsf{S} : H^1(\Gamma) \times L^2(\Gamma) \to H^1(\Omega_i)$, $\mathsf{S}(g_D, g_N) := u_i$ for (4) can be extended to a meromorphic function of $k \in \mathbb{C}$, which has poles only below the real axis in $\{z \in \mathbb{C}, \operatorname{Im} z < 0\}$ [27, Appendix A], [36]. From [27, Section 6.1] and [30] we learn that in the case $n_i > 1$ and for smooth $\Gamma$ there is a sequence of poles $(k_j)_{j=1}^\infty$ with real parts $\to \infty$ and $|\operatorname{Im} k_j| \leq C_p |\operatorname{Re} k_j|^{-p}$ for any $p \in \mathbb{N}$. We conclude that in high-frequency settings those poles can come arbitrarily close to the real axis.

For a wave number for which a pole happens to be close to the real axis, there will occur "almost" eigenvalue-eigenvector pairs, also known as quasi-resonances and quasi-modes. These modes correspond to the so-called whispering-gallery modes [27, Sect. 6.2], which are strong (in the sense of a large $H^1(\Omega_i)$-norm) fields localised near the interface. Those have been widely studied in the context of asymptotic analysis, see [6, 33, 35], the review paper [7] and the book [4].

*Remark* 1. For $d = 2$ the model (4) can also be used for electromagnetic scattering with translation invariance in one direction. It is then called TE (transversal electric) or TM (transversal magnetic) model and $u$ stands for a single component of either the electric or magnetic field, *cf.* [27, Remark 2.5].

*Remark* 2. In computational elastodynamics the model (4) is known and used as "acoustic approximation", see [10, Section 1.2.6].

1.2. **Outline and main results.** In this work we propose and study a numerical method for the detection of quasi-resonances. We first recast the transmission problem (4) as a second-kind direct boundary integral equation system posed in $L^2(\Gamma) \times L^2(\Gamma)$, see Section 2. The idea is to inspect the smallest singular value $\sigma_{\min}$ of the resulting Fredholm operator as a function of $k$ and find wave numbers, for which $k \mapsto \sigma_{\min}(k)$ has a (local) minimum.

Of course, we can only approximately compute $\sigma_{\min}$ and we do this by relying on a Galerkin boundary-element discretization employing low-order piecewise polynomial subspaces of $L^2(\Gamma) \times L^2(\Gamma)$. The method is explained in Section 3 and an analysis of the $h$-convergence of singular values computed for the Galerkin matrices is given in Section 4. In this section we develop a general a-priori estimation theory for approximating singular values of Fredholm operators, which may be of independent interest. The technique is based on the well-established Babuska-Osborn theory [5], and so leaves open the standard path to the development of a posteriori error estimators and adaptive approximation schemes.

The function $k \mapsto \sigma_{\min}(k)$ may have numerous and also shallow minima in any $k$-interval. To find them we devise a bespoke sampling-based adaptive bisection-type root-finding algorithm outlined in Section 5. This method employs a number of heuristics and, of course, offers no guarantee for detecting all minima. We hope that the benchmark numerical tests reported in Section 6 convince the reader that our algorithm is viable and fairly reliable in practical settings.

Finally, we caution that the possible occurrence of spurious quasi-resonances [20] limits the applicability of this idea to the case $n_i > 1$, see Remark 3.

1.3. **Relevance and related work.** In fact, this work was motivated by the discussion of plasmonic scatterers from [24]. Indeed, plasmonics is a field, where quasi-resonances leading to local field enhancement are of paramount importance. More generally, quasi-resonances are a central concern for many wave propagation phenomena modeled in computational engineering: either they are desired or should be avoided. In both cases, they have to be detected in numerical simulations and our method serves this purpose.

We point out that two main alternative approaches have been investigated:

(i) An important class are *contour integral methods* based on analytic Fredholm theory [3, 8, 38, 39], which yield approximations of the resonance poles in predefined regions of the complex plane. This is the basis for the FEAST algorithm [14] and the recursive-subdivision technique [21], applied to transmission problems, for instance, in [26].

(ii) Another class of methods aims to approximate $k$-dependent quantities including eigenvalues/singular values by means of *rational functions* with poles in the complex plane [23, 31].

These approaches explicitly rely on *complex-analysis* techniques. Conversely, we do not try to find the poles of the meromorphic extension of the solution operator, but exclusively rely on its norm for *real* wave numbers $k$ in an interval. This sets this article apart from the works mentioned above. What remains to be done is a thorough comparison of the methods, which is beyond the scope of the present paper.

## 2. Boundary Integral Equations

Assume that $u_* \in H^1_{\mathrm{loc}}(\Omega_*)$, $* = i, o$, solves $(\Delta + k^2 n_*)u = 0$ in $\Omega_*$ and complies with the Sommerfeld radiation conditions for $* = o$ (a "radiating solution" in this case). Then from [32, Section 3.1.13] and [25, Thm. 6.10] we learn the boundary potential representation formula

$$u_*(\boldsymbol{x}) = \int_\Gamma G_*(\kappa; \boldsymbol{x}-\boldsymbol{y})\gamma_N^* u_*(\boldsymbol{y})\,\mathrm{d}S(\boldsymbol{y}) - \int_\Gamma \mathbf{grad}\, G_*(\kappa; \boldsymbol{x}-\boldsymbol{y})\cdot \boldsymbol{\nu}_*(\boldsymbol{y})\,\gamma_D^* u_*(\boldsymbol{y})\,\mathrm{d}S(\boldsymbol{y})\,, \quad \boldsymbol{x}\notin\Gamma\,, \tag{5}$$

with the fundamental solution [32, Equ. (3.3)]

$$G_*(\kappa;\boldsymbol{z}) := \begin{cases} \frac{\imath}{4}H_0^{(1)}(\kappa\,\|\boldsymbol{z}\|) & \text{for } d=2\,,\\ \dfrac{\exp(\imath\kappa\,\|\boldsymbol{z}\|)}{4\pi\,\|\boldsymbol{z}\|} & \text{for } d=3\,, \end{cases} \qquad \boldsymbol{z}\in\mathbb{R}^d\setminus\{0\}\,, \quad \kappa := \begin{cases} k\sqrt{n_i} & \text{for } *=i\,,\\ k & \text{for } *=o\,, \end{cases} \tag{6}$$

where $H_0^{(1)}$ is a Hankel function of the first kind.

Applying traces to (5) yields direct boundary integral equations involving the continuous boundary integral operators (BIOs), here given through their integral representation for sufficiently regular argument functions ($* = i, o$) [32, Section 3.3] [1]

$$\text{(7a)}\quad \mathsf{V}_* : H^{-\frac{1}{2}}(\partial\Omega) \to H^{\frac{1}{2}}(\partial\Omega)\ , \qquad \mathsf{V}_*\varphi(\boldsymbol{x}) := \int_\Gamma G_*(\kappa;\boldsymbol{x}-\boldsymbol{y})\,\varphi(\boldsymbol{y})\,\mathrm{d}S(\boldsymbol{y})\ ,$$

$$\text{(7b)}\quad \mathsf{K}_* : H^{\frac{1}{2}}(\partial\Omega) \to H^{\frac{1}{2}}(\partial\Omega)\ , \qquad \mathsf{K}_* v(\boldsymbol{x}) := -\int_\Gamma \mathbf{grad}\, G_*(\kappa;\boldsymbol{x}-\boldsymbol{y})\cdot\boldsymbol{\nu}_*(\boldsymbol{y})\,v(\boldsymbol{y})\,\mathrm{d}S(\boldsymbol{y})\ ,$$

$$\text{(7c)}\quad \mathsf{K}'_* : H^{-\frac{1}{2}}(\partial\Omega) \to H^{-\frac{1}{2}}(\partial\Omega)\ , \qquad \mathsf{K}'_*\varphi(\boldsymbol{x}) := \int_\Gamma \mathbf{grad}\, G_*(\kappa;\boldsymbol{x}-\boldsymbol{y})\cdot\boldsymbol{\nu}_*(\boldsymbol{x})\,\varphi(\boldsymbol{y})\,\mathrm{d}S(\boldsymbol{y})\ ,$$

$$\text{(7d)}\quad \mathsf{W}_* : H^{\frac{1}{2}}(\partial\Omega) \to H^{-\frac{1}{2}}(\partial\Omega)\ , \qquad \mathsf{W}_* v(\boldsymbol{x}) := -\int_\Gamma \boldsymbol{\nu}_*(\boldsymbol{x})^\top \mathsf{D}^2 G_*(\kappa;\boldsymbol{x}-\boldsymbol{y})\boldsymbol{\nu}_*(\boldsymbol{y})\,v(\boldsymbol{y})\,\mathrm{d}S(\boldsymbol{y})\ ,$$

where the singular integrals in (7b) and (7c) are to be read in Cauchy sense, and those in (7d) in finite-part sense.

The inner product $(\cdot,\cdot)_{L^2(\Gamma)}$ of $L^2(\Gamma)$ induces a duality pairing on $H^{-\frac{1}{2}}(\partial\Omega)\times H^{\frac{1}{2}}(\partial\Omega)$, which makes it possible to associate a sesqui-linear form to every integral operator from (7). This paves the way for the following important regularization of the (variational) hypersingular boundary integral operator from (7d), see [32, Cor. 3.3.24] and [25, Ex. 9.6]: for all $u, v \in H^1(\Gamma)$

$$\text{(8)}\quad (\mathsf{W}_* u, v)_{L^2(\Gamma)} = \begin{cases} \int_\Gamma\int_\Gamma G_*(\kappa;\boldsymbol{x}-\boldsymbol{y})\left(\frac{du}{ds}(\boldsymbol{y})\,\frac{d\overline{v}}{ds}(\boldsymbol{x}) - \kappa^2\boldsymbol{\nu}_*(\boldsymbol{y})u(\boldsymbol{y})\boldsymbol{\nu}_*(\boldsymbol{x})\overline{v}(\boldsymbol{x})\right)\mathrm{d}S(\boldsymbol{y})\mathrm{d}S(\boldsymbol{x}), & d=2\ , \\ \int_\Gamma\int_\Gamma G_*(\kappa;\boldsymbol{x}-\boldsymbol{y})\left(\mathbf{curl}_\Gamma u(\boldsymbol{y})\cdot\mathbf{curl}_\Gamma\overline{v}(\boldsymbol{x}) - \kappa^2\boldsymbol{\nu}_*(\boldsymbol{y})u(\boldsymbol{y})\boldsymbol{\nu}_*(\boldsymbol{x})\overline{v}(\boldsymbol{x})\right)\mathrm{d}S(\boldsymbol{y})\mathrm{d}S(\boldsymbol{x}), & d=3\ , \end{cases}$$

where $\frac{d}{ds}$ stands for the arclength derivative along the curve $\Gamma$ ($d = 2$), and $\mathbf{curl}_\Gamma$ denotes the rotated surface gradient: $\mathbf{curl}_\Gamma w = \boldsymbol{\nu}_* \times \mathbf{grad}_\Gamma w$.

In particular, (5) combined with the jump relations [32, Section 3.3.1] yields a key characterization of pairs of traces of radiating solutions [11, Thm 2.6].

**Theorem 2.** *If and only if* $(v,\varphi) \in H^{\frac{1}{2}}(\Gamma)\times H^{-\frac{1}{2}}(\Gamma)$ *satisfies*

$$\text{(9)}\qquad \begin{bmatrix} \frac{1}{2}\mathsf{Id}+\mathsf{K}_* & -\mathsf{V}_* \\ -\mathsf{W}_* & \frac{1}{2}\mathsf{Id}-\mathsf{K}'_* \end{bmatrix}\begin{bmatrix} v \\ \varphi \end{bmatrix} = \begin{bmatrix} 0 \\ 0 \end{bmatrix}\ ,$$

*there exists a radiating solution* $u_* \in H^1_{\mathrm{loc}}(\Omega_*)$, $\Delta u_* + \kappa^2 u = 0$ *in* $\Omega_*$, *such that* $\gamma_D^* u_* = v$ *and* $\gamma_N^* u_* = \varphi$, $* = i, o$.

In particular this means for the traces of the solution $u$ of (4) and of the associated scattered field $u_s := u - u_{\mathrm{inc}}$:

$$\text{(10)}\qquad \begin{bmatrix} \frac{1}{2}\mathsf{Id}+\mathsf{K}_i & -\mathsf{V}_i \\ -\mathsf{W}_i & \frac{1}{2}\mathsf{Id}-\mathsf{K}'_i \end{bmatrix}\begin{bmatrix} \gamma_D^i u \\ \gamma_N^i u \end{bmatrix} = \begin{bmatrix} 0 \\ 0 \end{bmatrix}\ , \quad \begin{bmatrix} \frac{1}{2}\mathsf{Id}+\mathsf{K}_o & -\mathsf{V}_o \\ -\mathsf{W}_o & \frac{1}{2}\mathsf{Id}-\mathsf{K}'_o \end{bmatrix}\begin{bmatrix} \gamma_D^o u_s \\ \gamma_N^o u_s \end{bmatrix} = \begin{bmatrix} 0 \\ 0 \end{bmatrix}\ .$$

Next we use the transmission condition (4c) and (4d) to retain only the interior traces $\gamma_D^i u$ and $\gamma_N^i u$ of the total field. Then, following [12, 17], we add the resulting equations and get

$$\begin{bmatrix} \mathsf{Id}+(\mathsf{K}_o+\mathsf{K}_i) & \mathsf{V}_o-\mathsf{V}_i \\ \mathsf{W}_o-\mathsf{W}_i & \mathsf{Id}-(\mathsf{K}'_o+\mathsf{K}'_i) \end{bmatrix}\begin{bmatrix} \gamma_D^i u \\ \gamma_N^i u \end{bmatrix} = \begin{bmatrix} \frac{1}{2}\mathsf{Id}+\mathsf{K}_o & -\mathsf{V}_o \\ \mathsf{W}_o & -\frac{1}{2}\mathsf{Id}+\mathsf{K}'_o \end{bmatrix}\begin{bmatrix} \gamma_D^0 u_{\mathrm{inc}} \\ \gamma_N^0 u_{\mathrm{inc}} \end{bmatrix}\ .$$

[1] For boundary integral operators we suppress their $\kappa$-/$k$-dependence in the notation.

This leads to the following boundary integral equation for the unknown traces $v := \gamma_D^i u$ and $\varphi := \gamma_N^i u$:

$$(11)\quad (\mathsf{Id} + \mathsf{T}(k)) \begin{bmatrix} v \\ \varphi \end{bmatrix} = \begin{bmatrix} \frac{1}{2}\mathsf{Id} + \mathsf{K}_o & -\mathsf{V}_o \\ \mathsf{W}_o & -\frac{1}{2}\mathsf{Id} + \mathsf{K}_o' \end{bmatrix} \begin{bmatrix} \gamma_D^0 u_{\mathrm{inc}} \\ \gamma_N^0 u_{\mathrm{inc}} \end{bmatrix} \quad \text{with} \quad \mathsf{T}(k) := \begin{bmatrix} \mathsf{K}_o + \mathsf{K}_i & \mathsf{V}_o - \mathsf{V}_i \\ \mathsf{W}_o - \mathsf{W}_i & \mathsf{K}_o' + \mathsf{K}_i' \end{bmatrix} .$$

A key observation is that the sums and differences of boundary integral operators comprising $\mathsf{T}(k)$ cause a cancellation of the leading singularities of the integral kernels, because

$$(12)\qquad (G_o - G_i)(\boldsymbol{z}) = G_1(\boldsymbol{z}) + \|\boldsymbol{z}\| \, G_2(\boldsymbol{z}) \, ,$$

with entire functions $G_1, G_2 : \mathbb{R}^d \to \mathbb{C}$. Thus, in the same way as [19, Lemma 5] and [32, Thm 3.5.5] we can prove the following compactness result:

**Lemma 1.** *The compound boundary integral operator* $\mathsf{T}(k)$ *as defined in* (11) *is* compact *as both an operator* $\mathsf{T}(k) : H^{\frac{1}{2}}(\partial\Omega) \times H^{-\frac{1}{2}}(\partial\Omega) \to H^{\frac{1}{2}}(\partial\Omega) \times H^{-\frac{1}{2}}(\partial\Omega)$ *and* $\mathsf{T}(k) : L^2(\Gamma) \times L^2(\Gamma) \to L^2(\Gamma) \times L^2(\Gamma)$.

This means that for fixed wave number (11) is a direct *second-kind* boundary integral equation of the form $\mathsf{A}(k)U = F$, with a bounded linear operator

$$\mathsf{A}(k) : X \to X \quad , \quad \mathsf{A}(k) := \mathsf{Id} + \mathsf{T}(k) \, , \quad \mathsf{T}(k) : X \to X \quad \text{compact},$$

on a Hilbert space $X$. We can either choose $X := H^{\frac{1}{2}}(\partial\Omega) \times H^{-\frac{1}{2}}(\partial\Omega)$ or $X := L^2(\Gamma) \times L^2(\Gamma)$. In both cases $\mathsf{A}(k)$ will be a Fredholm operator of index zero [18, p. XI]. Thus, by means of a Fredholm alternative argument [37, Satz VI.2.4] we can establish existence and uniqueness of solutions.

**Theorem 3** ([27, Lemma 2.7])**.** *If* $u_{\mathrm{inc}} \in C^\infty(\mathbb{R}^d)$*, then the boundary integral equation* (11) *has a unique solution* $(v, \varphi) \in H^1(\Gamma) \times L^2(\Gamma)$.

Now we are in a position to give a rigorous definition of a near-resonance wave numbers.

**Definition 1.** *A wave number* $k > 0$ *is called* $\delta$*-near resonant for some* $\delta > 0$*, if*

$$\left\| (\mathsf{Id} + \mathsf{T}(k))^{-1} \right\|_{L^2(\Gamma) \to L^2(\Gamma)} \geq \delta^{-1} \, ,$$

*where* $\|\mathsf{Id} + \mathsf{T}(k)\|_0$ *is the operator norm of* $\mathsf{Id} + \mathsf{T}(k) : L^2(\Gamma) \times L^2(\Gamma) \to L^2(\Gamma) \times L^2(\Gamma)$.

The decision to rely on the Hilbert space $L^2(\Gamma)$ is motivated by the $L^2(\Gamma)$-setting used for discretization, see the next section.

*Example* 1. If $d = 2$ and $\Gamma$ is a circle, all boundary integral operators from (7) will be diagonalized by Fourier harmonics [1, Thm. 2], which also provide an orthonormal basis in $L^2(\Gamma)$. This permitted us to compute small singular values of $\mathsf{A}(k)$ and, thus, $\|\mathsf{A}(k)^{-1}\|_{L^2(\Gamma) \to L^2(\Gamma)}$, and plot them in Fig. 1 on the left.

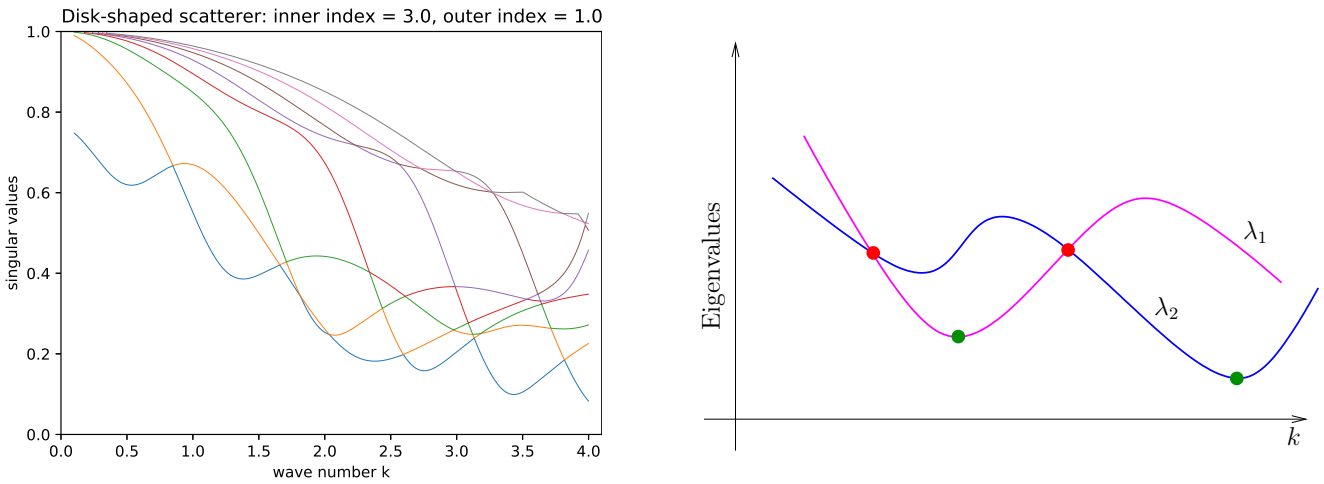


FIGURE 1. **Left**: A few of the smallest singular values of $\mathsf{A}(k)$ for scattering at unit disk, $n_i = 3$. The blue curve displays the smallest singular value $\sigma_{\min} = \|\mathsf{A}(k)\|^{-1}_{L^2(\Gamma)\to L^2(\Gamma)}$ as a function of $k$. The function $k \mapsto \sigma_{\min}(k)$ has numerous, but well-separated minima. **Right**: Qualitative rendering of possible graphs of $k \mapsto \lambda_i(\mathbf{W}(k))$ for the two smallest non-negative eigenvalues of $\mathbf{W}(k)$. Intersection points where $k \mapsto \min\{\lambda_1(k), \lambda_2(k)\}$ fails to be differentiable are marked with ●. Those intersection points cannot coincide with a minimum (marked with ●).

*Remark* 3 (Spurious quasi-resonances). Parallel to completing this manuscript some of the authors observed the phenomenon of *spurious quasi-resonances* affecting the second-kind boundary integral equation (11): The operator-valued meromorphic function $k \in \mathbb{C} \mapsto (\mathsf{Id} + \mathsf{T}(k))^{-1}$ can have poles in $\mathbb{C} \setminus \mathbb{R}$, where the solution operator of the transmission problem (4) has none. For a discrete set of wave numbers this can lead to large values of $\|(\mathsf{Id} + \mathsf{T}(k))^{-1}\|_{L^2(\Gamma)\to L^2(\Gamma)}$ though the mapping $(g_D, g_N) \to (u_i, u_s)$ from (4) well-conditioned at those $k$s.

An analysis is given in [20]. It shows that spurious quasi-resonances can be expected in the case $n_i < 1$, whereas in the case $n_i > 1$ they will not occur. Thus, the method proposed in this work should be applied only to settings with $n_i > 1$.

## 3. Boundary Element Galerkin Discretization

It goes without saying that we can only approximately compute $\|(\mathsf{Id} + \mathsf{T}(k))^{-1}\|_{L^2(\Gamma)\to L^2(\Gamma)}$ by means of a discrete model. We focus on Galerkin discretization. To begin with, let us revisit the abstract operator equation $\mathsf{A}(k)u = f$ on a Hilbert space $X$ introduced above. In order to perform Galerkin discretization we pick a finite-dimensional subspace $X_h \subset X$ and solve

$$u_h \in X_h : \quad (\mathsf{A}(k)u_h, v_h)_X = (f, v_h)_X \quad \forall v_h \in X_h \,, \tag{13}$$

where $(\cdot,\cdot)_X$ denotes the inner product in $X$. In the case of (11) the role of $\mathsf{A}(k)$ is played by $\mathsf{Id} + \mathsf{T}(k)$ for some $k > 0$ and we could choose $X := H^{\frac{1}{2}}(\partial\Omega) \times H^{-\frac{1}{2}}(\partial\Omega)$ or $X := L^2(\Gamma) \times L^2(\Gamma)$. However, the concrete $\mathsf{A}$ from (11) involves non-local boundary integral operators, which rules out the use of the non-local inner product of $H^{\frac{1}{2}}(\partial\Omega) \times H^{-\frac{1}{2}}(\partial\Omega)$, because this would lead to a computationally intractable scheme. Thus, Galerkin discretization in $X := L^2(\Gamma) \to L^2(\Gamma)$ remains the only option.

Then, based on a finite-dimensional trial/test space $X_h \subset X := L^2(\Gamma) \times L^2(\Gamma)$, $X_h = X_h^D \times X_h^N$, $X_h^D, X_h^N \subset L^2(\Gamma)$, and on the straightforward variational expression for $\mathsf{T}(k)$ in $L^2(\Gamma) \times L^2(\Gamma)$, we

arrive at the following variational characterization of the discrete operator $\mathsf{A}_h(k) : X_h \to X_h$.

$$\left(\mathsf{A}_h(k)\begin{bmatrix} v_h \\ \varphi_h \end{bmatrix}, \begin{bmatrix} v_h' \\ \varphi_h' \end{bmatrix}\right)_{L^2(\Gamma)\times L^2(\Gamma)} := (v_h, v_h')_{L^2(\Gamma)} + (\varphi_h, \varphi_h')_{L^2(\Gamma)} + ((\mathsf{K}_o + \mathsf{K}_i)v_h, v_h')_{L^2(\Gamma)} + ((\mathsf{V}_o - \mathsf{V}_i)\varphi_h, v_h')_{L^2(\Gamma)} + ((\mathsf{W}_o - \mathsf{W}_i)v_h, \varphi_h')_{L^2(\Gamma)} - ((\mathsf{K}_o' - \mathsf{K}_i')\varphi_h, \varphi_h')_{L^2(\Gamma)} \tag{14}$$

for all $v_h, v_h' \in X_h^D$, $\varphi_h, \varphi_h' \in X_h^N$. In a compact fashion, (14) can be expressed as

$$\mathsf{A}_h(k) = \mathsf{P}_h \mathsf{A}(k) \ , \tag{15}$$

with the $X$-orthogonal projection $\mathsf{P}_h : X \to X_h$ onto $X_h \subset X$.

After discretization, the search for near-resonant wavenumbers amounts to finding $k \in [k_{\min}, k_{\max}]$ such that $\left\|\mathsf{A}_h^{-1}(k)\right\|_{L^2(\Gamma)\to L^2(\Gamma)}$ is above a given threshold $\delta^{-1}$, $\delta > 0$. Equivalently, writing $\sigma_1(k) \geq \sigma_2(k) \geq \cdots \geq \sigma_{N-1}(k) \geq \sigma_N(k) \geq 0$ for the ordered *singular values* of $\mathsf{A}_h(k)$, we can use $\left\|\mathsf{A}_h^{-1}(k)\right\|_{L^2(\Gamma)\to L^2(\Gamma)} = \sigma_N^{-1}$ and examine, where $k \mapsto \sigma_N(k)$ drops below $\delta$.

In order to reduce the problem to numerical linear algebra we introduce a basis $\mathfrak{B} := \{b_1, \ldots, b_N\}$, $N := \dim X_h$, of $X_h$. Then the matrix $\mathbf{A}(k) \in \mathbb{C}^{N,N}$ representing $\mathsf{A}_h(k)$ in that basis is

$$\mathbf{A}(k) = \mathbf{M}^{-1}\mathbf{G}(k) \quad \text{with} \quad \mathbf{G}(k) := \left[(\mathbf{A}(k)b_j, b_k)_X\right]_{k,j=1}^N \ , \quad \mathbf{M} := \left[(b_j, b_k)_X\right]_{k,j=1}^N \ . \tag{16}$$

Note that $(\mathbf{A}(k)b_j, b_k)_X$ can be computed using (14) and that the Galerkin matrix $\mathbf{M} \in \mathbb{C}^{N,N}$ is Hermitian and positive definite. It can be used to introduce an orthonormal basis (ONB) $\widetilde{\mathfrak{B}} := \{q_1, \ldots, q_N\}$ of $X_h$ according to

$$q_j = \sum_{k=1}^N s_{j,k} b_k \quad \text{with} \quad [s_{j,k}]_{j,k=1}^N := \mathbf{L}^{-1} \ , \tag{17}$$

where $\mathbf{M} = \mathbf{L}\mathbf{L}^H$ is the Cholesky decomposition of $\mathbf{M}$, which means that $\mathbf{L} \in \mathbb{C}^{N,N}$ is lower triangular.

In the ONB $\widetilde{\mathfrak{B}}$ the operator $\mathsf{A}_h(k)$ has the matrix representation

$$\widetilde{\mathbf{A}}(k) = \mathbf{L}^H \mathbf{A}(k) \mathbf{L}^{-1} = \mathbf{L}^{-1}\mathbf{G}(k)\mathbf{L}^{-1} \ . \tag{18}$$

An ONB induces an isometric isomorphism between $X_h$ and the Euclidean space $\mathbb{C}^N$. Thus the singular values of $\mathsf{A}_h(k) : X_h \to X_h$ and those of the matrix $\widetilde{\mathbf{A}}(k) \in \mathbb{C}^{N,N}$ agree. This leads us to the following practical objective.

**Task (T).** *Find all minima of* $k \in [k_{\min}, k_{\max}] \mapsto \sigma_{\min}(\mathbf{L}^{-1}\mathbf{A}(k)\mathbf{L}^{-1})$ *with values* $\leq \delta$.

Our concrete choice of $X_h$ are low-degree boundary element spaces. To that end we equip $\Gamma$ with a triangulation $\mathcal{G} = \{K\}$ composed of (curved) segments ($d = 2$) or (curved) triangles ($d = 3$). Each of these so-called panels $K$ is obtained as the image of a reference interval $\widehat{K} := ]0, 1[$ ($d = 2$) or of a flat reference triangle $\widehat{K} \subset \mathbb{R}^2$ under a diffeomorphism $\mathbf{\Phi}_K : \widehat{K} \to K$. Following [32, Section 4.1.7] we introduce the space

$$\mathcal{S}_{\mathcal{G}}^{1,0} := \{v \in C^0(\Gamma) \,|\, \forall K \in \mathcal{G} : \, v \circ \mathbf{\Phi}_K \in \mathcal{P}^1(\mathbb{R}^{d-1})\} \ , \tag{19}$$

where $\mathcal{P}^k(\mathbb{R}^{d-1})$ is the space of $d-1$-variate polynomials of degree $\leq k$. For a detailed discussion of these parametric boundary element spaces refer to [32, Section 4.1]. Then, for Galerkin discretization we rely on

$$X_h := \mathcal{S}_{\mathcal{G}}^{1,0} \times \mathcal{S}_{\mathcal{G}}^{1,0} \quad \Leftrightarrow \quad X_h^D := X_h^N := \mathcal{S}_{\mathcal{G}}^{1,0} \ . \tag{20}$$

In the sequel, whenever we make statements about convergence, we will tacitly assume uniformly shape-regular sequences of triangulations $(\mathcal{G}_h)_h$ indexed by the mesh width $h$. In this setting the following approximation properties are easily established [32, Sect. 4.3]:

$$\exists C > 0 : \quad \inf_{v_h \in \mathcal{S}_h^{1,0}} \|v - v_h\|_{L^2(\Gamma)} \leq C h^{\min\{2,s\}} \|v\|_{H^s(\Gamma)} \quad \forall v \in H^s(\Gamma) , \quad \forall h . \tag{21}$$

*Remark* 4. Another natural and viable choice of trial and test spaces for the Galerkin discretization of (11) would be

$$X_h^D := \mathcal{S}_{\mathcal{G}}^{1,0} \quad , \quad X_h^N := \mathcal{S}_{\mathcal{G}}^{0,-1} , \tag{22}$$

where $\mathcal{S}_{\mathcal{G}}^{0,-1}$ is the space of $\mathcal{G}$-piecewise constants. We point out that (20) permits us to employ the convenient formula (8) since $X_h^D, X_h^N \subset H^1(\Gamma)$, whereas (22) denies this possibility.

*Remark* 5. For $d = 2$ and smooth $\Gamma$ spectral Galerkin discretization based on mapped Fourier harmonics offers a discretization of superior efficiency [17]. However, this advantage does not carry over to situations where $\Gamma$ has corners, causing local singularities of $\gamma_D^i u$ and $\gamma_N^i$, which will severely affect the convergence of spectral Galerkin schemes. Then low-degree boundary element spaces become competitive.

## 4. Approximating the Smallest Singular Value

Now we briefly review the approximation theory for estimating the singular values of a Fredholm operator $\mathsf{A} : X \to X$, $X$ a Hilbert space, of the form $\mathsf{A} = \mathsf{Id} + \mathsf{T}$, with $\mathsf{T} : X \to X$ compact. For a bounded linear operator $\mathsf{L} : X \to X$ we write $\mathrm{Spec}(\mathsf{A})$ for the spectrum of $\mathsf{L}$. An element of the spectrum is called essential if it is either an element of the continuous spectrum, an accumulation point of the spectrum or it is an eigenvalue of infinite multiplicity.

The singular values of $\mathsf{A}$ are defined as the eigenvalues of the operator $\sqrt{\mathsf{A}^*\mathsf{A}}$, where $\mathsf{A}^* : X \to X$ is the adjoint of $\mathsf{A}$. Here the square root is meant in the sense of the spectral calculus for self-adjoint bounded operators. By a direct computation it follows

$$\mathsf{A}^*\mathsf{A} = (\mathsf{Id} + \mathsf{T})^*(\mathsf{Id} + \mathsf{T}) = \mathsf{Id} + \mathsf{T}^* + \mathsf{T} + \mathsf{T}^*\mathsf{T} , \tag{23}$$

and so the operator $\mathsf{A}^*\mathsf{A}$ is also Fredholm. Consequently, the singular values of $\mathsf{A}$, which are the eigenvalues of $\sqrt{\mathsf{A}^*\mathsf{A}}$, accumulate at one. Therefore, the essential spectrum of $\sqrt{\mathsf{A}^*\mathsf{A}}$ is either empty or $\{1\}$, and every other element of $\mathrm{Spec}(\sqrt{\mathsf{A}^*\mathsf{A}})$ is an eigenvalue of finite multiplicity. Hence, we denote by

$$\sigma_{-1} \leq \sigma_{-2} \leq \cdots \leq \sigma_{-n} \leq \cdots < 1 < \cdots \leq \sigma_n \leq \cdots \leq \sigma_2 \leq \sigma_1$$

all the elements of $\mathrm{Spec}(\sqrt{\mathsf{A}^*\mathsf{A}}) \setminus \{1\}$. These are all singular values of $\mathsf{A}$ different from 1. Here we have used the eigenvalue counting convention of Parlett [29], where all eigenvalues are counted according to their multiplicity and eigenvalues in the lower part of the spectrum are counted with negative indices and the eigenvalues on the upper part of the spectrum are counted with positive indices. They have the standard variational characterization by the variational theorem for eigenvalues of bounded self-adjoint operators which are below/above the infimum/supremum of the essential spectrum. In particular, for $\sigma_{-i} < 1$ we have

$$\sigma_{-i} = \inf_{\substack{\mathcal{U}, \\ \dim(\mathcal{U})=i}} \sup_{u \in \mathcal{U}\setminus\{0\}} \frac{\|\mathsf{A}u\|_X}{\|u\|_X} , \tag{24}$$

and for $\sigma_i > 1$ the variational characterization reads

$$\sigma_i = \sup_{\substack{\mathcal{U}, \\ \dim(\mathcal{U})=i}} \inf_{u \in \mathcal{U} \setminus \{0\}} \frac{\|\mathsf{A}u\|_X}{\|u\|_X} \, . \tag{25}$$

*Remark* 6. Note that every statement we make has a counterpart for the eigenvalues in the upper part of the spectrum, where we count from the largest eigenvalue towards one.

Before we proceed let us define the Jordan-Wielandt block operator

$$\mathsf{W} := \begin{bmatrix} 0 & \mathsf{A} \\ \mathsf{A}^* & 0 \end{bmatrix} : X \times X \to X \times X \, . \tag{26}$$

This defines self-adjoint operator and

$$\mathrm{Spec}(\mathsf{W}) \setminus \{0\} = \{\sigma \ : \ \sigma \in \mathrm{Spec}(\sqrt{\mathsf{A}^*\mathsf{A}})\} \cup \{-\sigma \ : \ \sigma \in \mathrm{Spec}(\sqrt{\mathsf{A}^*\mathsf{A}})\} \, . \tag{27}$$

Furthermore, an eigenvalue $\lambda \in \mathrm{Spec}(\mathsf{W}) \setminus \{0\}$ has the same multiplicity as the eigenvalue $|\lambda| \in \mathrm{Spec}(\sqrt{\mathsf{A}^*\mathsf{A}})$.

To study the convergence of singular values in the context of Galerkin discretization, we assume that we are given a family $\{X_h\}_{h \in \mathbb{H}}$ of subspaces $X_h \subset X$, $\mathbb{H} \subset \mathbb{R}^+$ an index set with only accumulation point 0. If the $X_h$ are low-degree boundary element spaces as introduced in Section 3, $h$ could mean the mesh width of the underlying partition of $\Gamma$. We assume that the family $\{X_h\}_{h \in \mathbb{H}}$ is asymptotically dense in $X$:

$$\forall u \in X : \quad \lim_{h \in \mathbb{H} \to 0} \inf_{v_h \in X_h} \|u - v_h\| = 0 \, . \tag{28}$$

Writing $\mathsf{P}_h : X \to X_h$ for the orthogonal projections onto $X_h$, the discrete operators $\mathsf{A}_h : X_h \to X_h$, $h \in \mathbb{H}$, are defined as

$$\mathsf{A}_h := \mathsf{P}_h \circ \mathsf{A} : X_h \to X_h \, . \tag{29}$$

We call $\mathsf{A}_h$ the Ritz-Galerkin discretization of $\mathsf{A}$. Sometimes, without further mention, we regard it as an operator on $X$: $\mathsf{A}_h := \mathsf{P}_h \circ \mathsf{A} \circ \mathsf{P}_h : X \to X$ We now state a convergence result for its singular values.

**Theorem 4.** *Let $-1 < \cdots \leq -\sigma_{-i} \leq \cdots \leq -\sigma_1 < 0 < \sigma_{-1} \leq \cdots \leq \sigma_{-n} < \cdots < 1$ be the eigenvalues of the operator $\mathsf{W}$ with modulus strictly less than one. Let also $\sigma_{h,-i}$ and $-\sigma_{h,-i}$ be the eigenvalues of the block operator*

$$\mathsf{W}_h = \begin{bmatrix} 0 & \mathsf{A}_h \\ \mathsf{A}_h^* & 0 \end{bmatrix} : X_h \times X_h \to X_h \times X_h \, ,$$

*which are in absolute values strictly less than one. Then*

$$\lim_{h \to 0} |\sigma_{-i} - \sigma_{h,-i}| = 0 \, ,$$

*where we have counted the eigenvalues according to multiplicity. An equivalent result holds for all eigenvalues of $\mathsf{W}_h$ which are strictly larger than one in absolute value.*

*Proof.* The first claim of the theorem follows directly as in [28]. Note that

$$\begin{aligned} \|\mathsf{W} - \mathsf{W}_h\| &= \left\| \begin{bmatrix} 0 & \mathsf{A} - \mathsf{A}_h \\ \mathsf{A}^* - \mathsf{A}_h^* & 0 \end{bmatrix} \right\| \\ &= \left\| \begin{bmatrix} 0 & (\mathsf{Id} - \mathsf{P}_h)\mathsf{T} + \mathsf{P}_h\mathsf{T}(\mathsf{Id} - \mathsf{T}_h) \\ \mathsf{T}^*(\mathsf{Id} - \mathsf{P}_h) + (\mathsf{Id} - \mathsf{P}_h)\mathsf{T}^*\mathsf{P}_h & 0 \end{bmatrix} \right\| \\ &= \|(\mathsf{Id} - \mathsf{P}_h)\mathsf{T} + \mathsf{P}_h\mathsf{T}(\mathsf{Id} - \mathsf{P}_h)\| \, . \end{aligned}$$

Since, thanks to (28), $\mathsf{Id} - \mathsf{P}_h$ converges to zero strongly for $h \to 0$, and $\mathsf{T}$ is compact, then $\|\mathsf{W} - \mathsf{W}_h\|_{X\times X \to X\times X} \to 0$ [22, Cor. 10.4]. Note that here, as before, we have concisely written $\mathsf{P}_h \circ \mathsf{T} \circ \mathsf{P}_h = \mathsf{P}_h\mathsf{T}\mathsf{P}_h$. Since norm convergence of bounded operators implies the norm convergence of the resolvent, it follows that the eigenvalues of $\mathsf{W}_h$ converge with multiplicity to the eigenvalues of $\mathsf{W}$ and that spectral projections of $\mathsf{W}_h$ converge in norm to the spectral projections of $\mathsf{W}$. Note that with this we have also proved the claim for all eigenvalues of finite multiplicity of $\mathsf{W}$, and so in particular also for those which are in absolute value strictly larger than one. □

**Corollary 1.** *Using the notations from Theorem 4, let $u_i, v_i \in X$ be nonzero unit vectors such that $\mathsf{A}u_i = \sigma_i v_i$. Then for $h$ small enough we can choose nonzero unit vectors $u_{h,i}$, $v_{h,i}$ such that $\mathsf{A}_h u_{h,i} = \sigma_{h,i} v_{h,i}$ and*

$$\|u_i - u_{h,i}\| + \|v_i - v_{h,i}\| \to 0 \quad \textit{for} \quad h \to 0 \,.$$

**Theorem 5.** *Adopt the notations of Theorem 4. Then for $h$ small enough the singular values $\sigma_{h,j}$, $\sigma_j$, $|\sigma_j| \neq 1$, verify (with $C > 0$ independent of $h$)*

$$|\sigma_j - \sigma_{h,i}| \leq C\|(\mathsf{Id} - \mathsf{P}_h)\big|_{E(\sigma_j)}\|^2, \qquad i = 1, \ldots, q \,.$$

*Here $E(\sigma_j)$ is the spectral subspace belonging to $\sigma_j$ as an eigenvalue of the Jordan-Wielandt matrix and $q < \infty$ is the multiplicity of $\sigma_j$.*

*Proof.* Recall that

$$\mathsf{W} = \begin{bmatrix} 0 & \mathsf{Id} + \mathsf{T} \\ \mathsf{Id} + \mathsf{T}^* & 0 \end{bmatrix}, \qquad \mathsf{W}_h = \begin{bmatrix} 0 & \mathsf{Id} + \mathsf{P}_h\mathsf{T}\mathsf{P}_h \\ \mathsf{Id} + \mathsf{P}_h\mathsf{T}^*\mathsf{P}_h & 0 \end{bmatrix}$$

and then

$$\mathsf{W} - \mathsf{W}_h = \begin{bmatrix} 0 & \mathsf{T} - \mathsf{P}_h\mathsf{T}\mathsf{P}_h \\ \mathsf{T}^* - \mathsf{P}_h\mathsf{T}^*\mathsf{P}_h & 0 \end{bmatrix}$$

is a compact operator and

$$\inf_{\tilde{u}\in \mathrm{Ran}(\mathsf{P}_h)} \|u - \tilde{u}\|^2 = \|(\mathsf{Id} - \mathsf{P}_h)u\|^2 \,.$$

Let further $\mathsf{A}u_i = \sigma_j v_i$ and $\mathsf{A}^* v_i = \sigma_j u_i$, for $i = 1, \cdots, q$. We can choose $u_i$ and $v_i$, $i = 1, \cdots, q$ so that the eigenspace $E(\sigma_j)$ of $\mathsf{W}$ associated to $\sigma_j$ is represented by a basis of eigenvectors

$$E(\sigma_j) = \mathrm{span}\Big\{ \begin{bmatrix} v_i \\ u_i \end{bmatrix}, \, i = 1, \cdots, q \Big\} \,.$$

We will assume that the product space $L^2(\Gamma) \times L^2(\Gamma)$ is equipped with the natural scalar product and we will use the abbreviated notation

$$v \oplus u := \begin{bmatrix} v \\ u \end{bmatrix} \in L^2(\Gamma) \times L^2(\Gamma)$$

to denote its elements. In particular, by $\psi_i = v_i \oplus u_i$, $i = 1, \cdots, q$, we denote the chosen basis for $E(\sigma_j)$.

The technique of [5, 28] implies for an eigenvalue of multiplicity $q < \infty$ below/above the infimum/supremum of the essential spectrum and $h$ small enough

$$\begin{aligned} |\sigma_j - \sigma_{h,i}| &\leq C\Big\{ \sum_{p,k=1}^{q} |((\mathsf{W} - \mathsf{W}_h)\psi_p, \psi_k)| + \|(\mathsf{W} - \mathsf{W}_h)\Big|_{E(\sigma_j)}\|^2 \Big\} \\ &= C\Big\{ \sum_{p,k=1}^{q} |((\mathsf{W} - \mathsf{W}_h)\psi_p, \psi_k)| + \| \begin{bmatrix} 0 & \mathsf{T} - \mathsf{P}_h\mathsf{T}\mathsf{P}_h \\ \mathsf{T}^* - \mathsf{P}_h\mathsf{T}^*\mathsf{P}_h & 0 \end{bmatrix} \Big|_{E(\sigma_j)}\|^2 \Big\} \end{aligned}$$

and $i = 1, \cdots, q$. In this context $h$ is small enough if the matching from Corollary 1 holds.

For any $\psi_p = v_p \oplus u_p$, $\psi_k = v_k \oplus u_k$, $p, k = 1, \cdots q$, we compute

$$\begin{aligned}|((\mathsf{W} - \mathsf{W}_h)\psi_p, \psi_k)| &= |\Big( \begin{bmatrix} 0 & \mathsf{T} - \mathsf{P}_h\mathsf{T}\mathsf{P}_h \\ \mathsf{T}^* - \mathsf{P}_h\mathsf{T}^*\mathsf{P}_h & 0 \end{bmatrix} \psi_p, \psi_k\Big)| \\ &|((\mathsf{T} - \mathsf{P}_h\mathsf{T}\mathsf{P}_h)u_p, v_k) + ((\mathsf{T}^* - \mathsf{P}_h\mathsf{T}^*\mathsf{P}_h)v_p, u_k)| \\ &\leq |((\mathsf{T} - \mathsf{P}_h\mathsf{T}\mathsf{P}_h)u_p, v_k)| + |((\mathsf{T}^* - \mathsf{P}_h\mathsf{T}^*\mathsf{P}_h)v_p, u_k)| \ .\end{aligned}$$

Obviously,

$$\mathsf{T} - \mathsf{P}_h\mathsf{T}\mathsf{P}_h = \mathsf{T} - \mathsf{P}_h\mathsf{T} + \mathsf{P}_h\mathsf{T}(\mathsf{Id} - \mathsf{P}_h)$$

and so, for any $\eta_1, \eta_2 \in \mathrm{Ran}(\mathsf{P}_h)$,

$$\begin{aligned}|((\mathsf{T} - \mathsf{P}_h\mathsf{T}\mathsf{P}_h)u_p, v_k)| &= |((\mathsf{T} - P_\mathsf{T}\mathsf{T} + P_\mathsf{T}\mathsf{T}(\mathsf{Id} - P_\mathsf{T}))u_p, v_k)| \\ &\leq |((\mathsf{T} - \mathsf{P}_h\mathsf{T})u_p, v_k)| + |(\mathsf{P}_h\mathsf{T}(\mathsf{Id} - \mathsf{P}_h))u_p, v_k)| \\ &= |((\mathsf{T} - \mathsf{P}_h\mathsf{T})u_p, v_k + \eta_1)| + |(\mathsf{P}_h\mathsf{T}(\mathsf{Id} - \mathsf{P}_h))u_p + \eta_2, v_k)| \\ &\leq \|(\mathsf{T} - \mathsf{P}_h\mathsf{T})u_p\|\|v_k + \eta_1\| + \|\|u_p + \eta_2\|\|((\mathsf{Id} - \mathsf{P}_h)\mathsf{T}^*\mathsf{P}_h)v_k\| \ .\end{aligned}$$

This implies

$$|((\mathsf{T} - \mathsf{P}_h\mathsf{T}\mathsf{P}_h)u_p, v_k)| \leq \|(\mathsf{Id} - \mathsf{P}_h)\mathsf{T}u_p\|\|(\mathsf{Id} - \mathsf{P}_h)v_k\| + \|(\mathsf{Id} - \mathsf{P}_h)u_p\|\|(\mathsf{Id} - \mathsf{P}_h)\mathsf{T}^*\mathsf{P}_h v_k\|,$$

since the inequality holds for any $\eta_1, \eta_2 \in \mathrm{Ran}(\mathsf{P}_h)$. The estimate for the dual operator follows analogously. Finally,

$$\|(\mathsf{T} - \mathsf{P}_h\mathsf{T}\mathsf{P}_h)u_p\| \leq \|(\mathsf{Id} - \mathsf{P}_h)\mathsf{T}u_p\| + \|\mathsf{P}_h\mathsf{T}(\mathsf{Id} - \mathsf{P}_h)u_p\| \ ,$$

and, equivalently, for the dual operator, allow us to complete the proof. Finally, note that $\mathsf{A}u_j = \sigma_j v_j$ and so, $\mathsf{T}u_j = \sigma_j v_j - u_j$ and equivalently $\mathsf{T}^* v_j = \sigma_j u_j - v_j$ allow us to conclude about the regularity of $\mathsf{T}u_p$ and $\mathsf{T}^* v_p$. The constant $C$ obviously depends on the regularity properties of functions from $E(\sigma_j)$. □

The best approximation in $X_h$ of elements in the low-dimensional spaces $E(\sigma_j)$ will determine the accuracy of the approximate singular values. In the context of the considered BEM this means that the smoothness of the singular functions in $E(\sigma_j)$ will govern convergence for mesh width $h \to 0$. The smoothness of singular functions will depend on the smoothness of the interface $\Gamma$. For smooth $\Gamma$ we expect smooth singular functions in $H^2(\Gamma)$ and then Theorem 5 together with (21) will lead to the optimal asymptotic convergence

$$|\sigma_j - \sigma_{h,i}| = O(h^4) \quad \text{for} \quad h \to 0 \tag{30}$$

on sequences of shape-regular triangulations. In case $\Gamma$ has corners (and edges for $d = 3$), the singular functions can even be discontinuous and rates of convergence will deteriorate unless locally refined triangulations are employed.

*Example* 2 (Convergence of singular values). As a test case we choose $\Omega_i := ]0, 1[^2$ as the unit square in 2D, the interior index of refraction $n_i = 3$, and a sequence of uniform triangulations of $\Gamma := \partial\Omega_i$ consisting of $N \in \{48, 96, 192, 384, 768\}$ panel (line segments) of equal length. We use the boundary-element space $X_h := \mathcal{S}^{1,0}_\mathcal{G} \times \mathcal{S}^{1,0}_\mathcal{G}$, see Section 3. The smallest ten singular values as a function of $k$ and computed with different mesh resolutions are shown in Fig. 2. We monitor the error in the smallest four singular values using those obtained for $N = 1536$ panels as reference. The results for four different wave numbers are plotted in Fig. 3

The measured rate of algebraic convergence remains far below 4, because some singular functions will even be unbounded at the corners of the square.

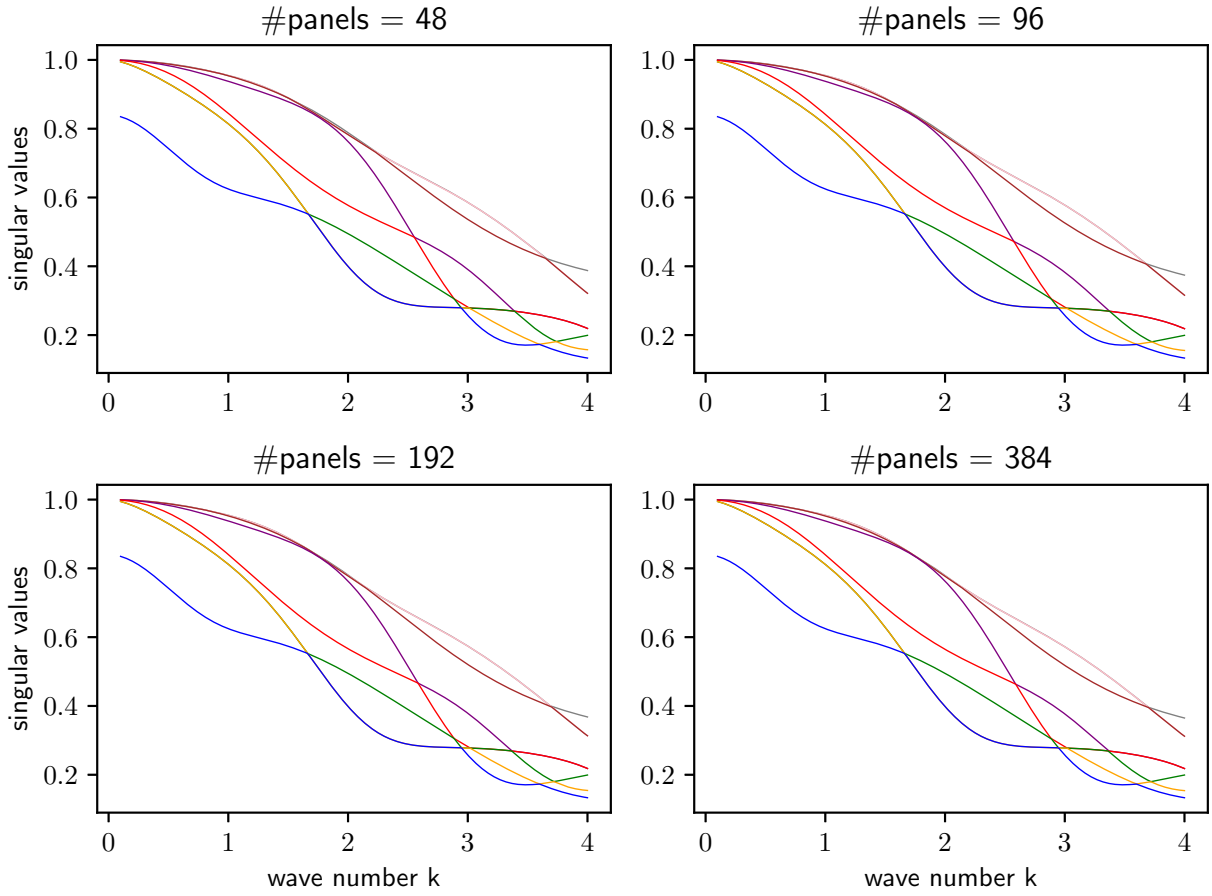


FIGURE 2. Galerkin BEM approximations of the ten smallest singular values of the transmission boundary integral operator and for unit square $\Omega_i$ and $k \in [0.1, 4]$. The singular values were computed with Arnoldi's method of Arpack using a very tight tolerance of $10^{-16}$.

## 5. Finding Near-Resonant Frequencies

As we have seen in Section 4 instead of the singular values of the matrix $\widetilde{\mathbf{A}}(k)$ we can examine the eigenvalues of the Hermitian *Wielandt matrix*

$$\mathbf{W}(k) := \begin{bmatrix} \mathbf{O} & \widetilde{\mathbf{A}}(k) \\ \widetilde{\mathbf{A}}(k)^H & \mathbf{O} \end{bmatrix} \in \mathbb{C}^{2N,2N} , \tag{31}$$

because (27) still holds:

$$\mathrm{Spec}(\mathbf{W}(\mathsf{k})) \setminus \{0\} = \{\sigma \ : \ \sigma^2 \in \mathrm{Spec}(\mathbf{A}(k)^H \mathbf{A}(k))\} . \tag{32}$$

Therefore we can reformulate Task (T) as follows:

**Task (TM).** *Given* $0 < k_{\min} < k_{\max}$ *find all minima of*

$$k \in [k_{\min}, k_{\max}] \mapsto \varphi(k) := \min\{\sigma \in \mathrm{Spec}(\mathbf{W}(k)), \, \sigma \geq 0\} \tag{33}$$

*with values* $\leq \delta$.

**Lemma 2** (Properties of $\varphi$)**.** *There is* $m \in \mathbb{N}$ *and a partition* $k_{\min} = \kappa_0 < \kappa_1 < \cdots < \kappa_{m-1} < \kappa_m = k_{\max}$ *of the interval* $[k_{\min}, k_{\max}]$ *such that the restriction of the function* $\varphi : [k_{\min}, k_{\max}] \to \mathbb{R}_0^+$,

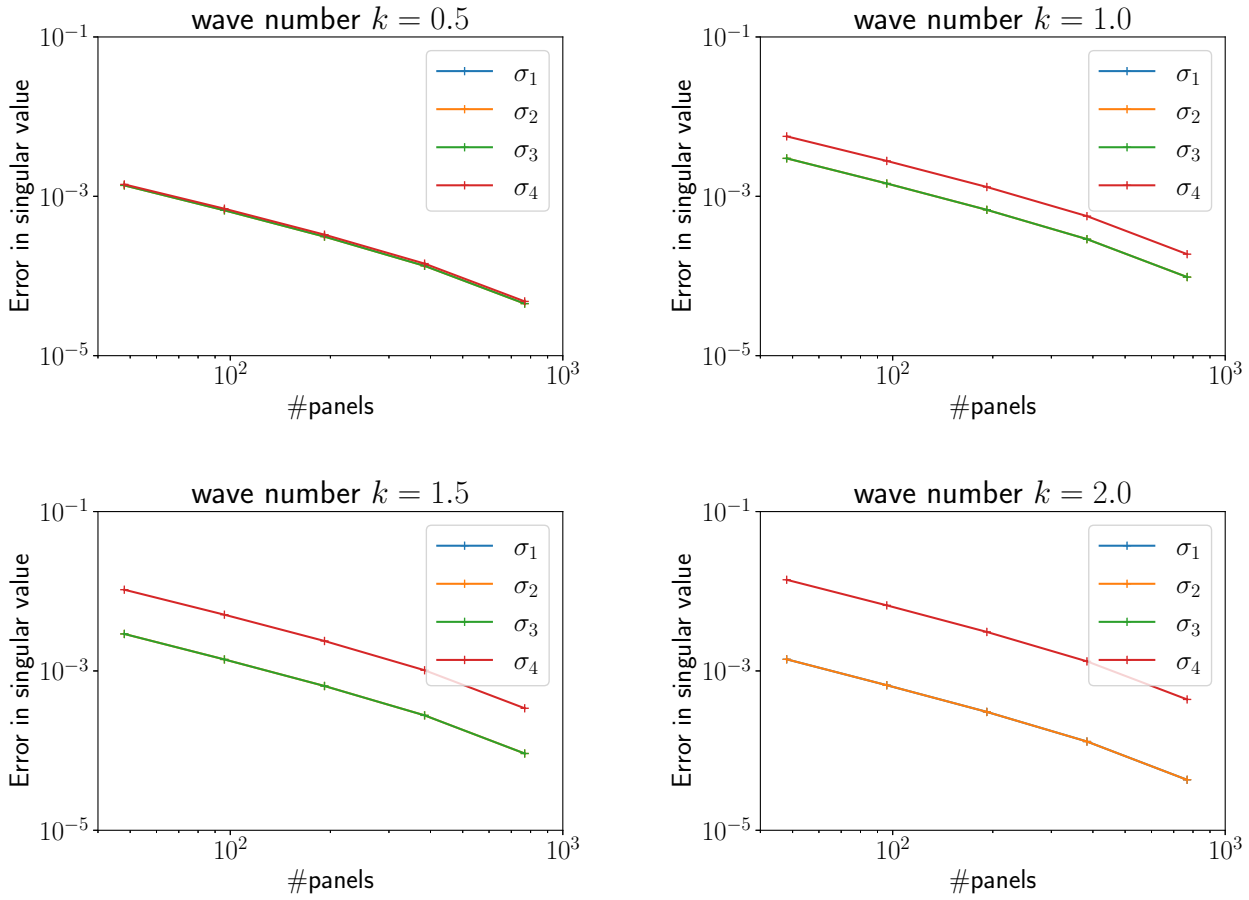


FIGURE 3. Scattering at the unit square with $n_i = 3$, $n_o = 1$ and four different wave numbers: Approximate errors in the four smallest singular values as approximated by Galerkin BEM and piecewise linear continuous trial and test functions, reference solution obtained with $N = 1536$ panels. In all cases we observe algebraic convergence $O(h^\alpha)$ for $h \sim N^{-1} \to 0$ with rate $\alpha \approx 1.2$. Symmetry makes two singular values agree. Therefore only two error curves are displayed in each plot.

$\varphi(k) := \min\{\sigma \in \mathrm{Spec}(\mathbf{W}(k)), \sigma \geq 0\}$, *to every interval* $]\kappa_{j-1}, \kappa_j[$, $j = 1, \ldots, m$, *belongs to* $C^\infty([\kappa_{j-1}, \kappa_j])$.

*Proof.* To begin with we note that $k \mapsto \mathbf{A}(k)$ is analytic on $\mathbb{R}^+$. As a consequence, the Wielandt matrix $\mathbf{W}(k)$ from (31) depends smoothly on $k$ and this will also carry over to its $2N$ eigenvalues (counted with multiplicity), assuming a suitable ($k$-dependent!) ordering. This renders $k \mapsto \varphi(k)$ the minimum of $N$ smooth functions. As such it is continuous and piecewise smooth with possible kinks at crossings of eigenvalues, see Fig. 1, right, for an illustration. □

The behavior of the non-negative eigenvalues of $k \mapsto \mathbf{W}(k)$, which agree with the singular values of $\widetilde{\mathbf{A}}(k)$ expressed in Lemma 2 is conspicuous in Fig. 1: Though singular values may change positions in the sorted sequence, they obviously lie on smooth curves, which matches mathematical results about the smooth dependence of singular values of matrices that are analytic functions of a parameter [9, Sect. 2]. We conclude that $\varphi$ must be smooth in every minimum, see Fig. 1, right for a visual justification. This makes it possible to tackle Task (TM) by searching zeros of $\varphi' := \frac{d\varphi}{dk}$.

**Task (TZ).** *Given* $0 < k_{\min} < k_{\max}$ *find the set*

$$\Theta := \{k \in ]k_{\min}, k_{\max}[ : \varphi \text{ differentiable in } k,\ \varphi'(k) = 0\} .$$

5.1. **Root finding.** In Listing 1 we outline[2] a *heuristic* adaptive subdivision algorithm for finding the roots of $\varphi'$ in $[k_{\min}, k_{\max}]$. The algorithm builds a partition of $[k_{\min}, k_{\max}]$ as an ordered sequence $\mathcal{S} = (k_{min} = \kappa_0 < \kappa_1 < \ldots < \kappa_{n-1} < \kappa_n = k_{\max})$, $n \in \mathbb{N}$, of knots $\kappa_i$ representing interval boundaries. Each interval is either flagged as Active, Zero, or NoZero, which indicates whether it still has to be processed or has already been identified as containing or not containing a zero of $\varphi'$.

The idea underlying Line 29–Line 41 of the code is to replace $\varphi'$ on small intervals with a cubic Hermite polynomial interpolant $p \in \mathcal{P}_3$, $\mathcal{P}_d$ the space of univariate polynomials of degree $\leq d$, as a surrogate function. The zeros of $p$ or, in case there are none, extrema of $p$ with small modulus will the be used to further subdivide the interval. If $p$ does not come close to zero on a small interval, we decide that there is no zero inside.

From Lemma 2 we know that $\varphi'$ can have jump discontinuities. In Line 20–Line 27 of Listing 1 we decide that the sign change of $\varphi'$ in an interval is probably due to a jump when the slope of $\varphi'$ predicted by a finite-difference approximation is much larger than the modulus of $\varphi''$ at the endpoints. Otherwise we conclude from a sign change of $\varphi'$ on a small interval that there is exactly one zero.

The decisions made in the algorithm depend on a few parameters marked magenta in Listing 1. These parameters have to be set by the user and we found suitable values by varying the parameters until we achieved maximum robustness of the algorithm for the test cases reported in Section 6.

5.2. **Computing derivatives of $\varphi$.** We fix $k > 0$ and tag derivatives with respect to $k$ with a prime $'$. We assume that $\lambda(k)$ is an eigenvalue of the Wielandt matrix $\mathbf{W}(k) \in \mathbb{C}^{2N,2N}$ *with multiplicity* 1. So there is a normalized eigenvector $\mathbf{u}(k) \in \mathbb{C}^{2N}$, unique up to sign, such that

$$\mathbf{W}(k)\mathbf{u}(k) = \lambda(k)\mathbf{u}(k) , \quad \mathbf{u}(k)^H\mathbf{u}(k) = 1 . \tag{34}$$

We differentiate both sides with respect to $k$:

$$\mathbf{W}'(k)\mathbf{u}(k) + \mathbf{W}(k)\mathbf{u}'(k) = \lambda'(k)\mathbf{u}(k) + \lambda(k)\mathbf{u}'(k) . \tag{35}$$

Left multiplying with $\mathbf{u}(k)^H$, using $\|\mathbf{u}(k)\| = 1$ and (34) we arrive at a compact expression for the first derivative of $k \mapsto \lambda(k)$ in $k$

$$\lambda'(k) = \mathbf{u}(k)^H\mathbf{W}(k)\mathbf{u}(k) . \tag{36}$$

Differentiating $\|\mathbf{u}(k)\|^2 = 1$ we conclude $\mathbf{u}'(k)^H\mathbf{u}(k) + \mathbf{u}(k)^H\mathbf{u}'(k) = 0$. Thus from (35) we can recover the derivative of the eigenvector as the solution of the augmented linear system of equations

$$\begin{aligned} (\mathbf{W}(k) - \lambda(k)\mathbf{I})\mathbf{u}'(k) + \mu\mathbf{u}(k) &= \lambda'(k)\mathbf{u}(k) - \mathbf{W}'(k)\mathbf{u}(k) , \\ \mathbf{u}(k)^H\mathbf{u}'(k) &= 0 , \end{aligned} \tag{37}$$

where $\mu \in \mathbb{R}$ is a Lagrange multiplier as an extra unknown. Note that the matrix $\mathbf{W}(k) - \lambda(k)\mathbf{I}$ is singular, but the system matrix of the $(2N+1) \times (2N+1)$ linear system of equations (37) is regular, because we assumed that $\lambda(k)$ has multiplicity 1. In addition, thanks to (36), we find $\mu = 0$.

[2]Some details of the algorithm have been omitted, in particular the treatment of special cases.

LISTING 1. Zero finding for $\varphi'$ (outline)

```
seq<real> findZeros(k_min, k_max) {
  seq<real> S := {κ_j := a + j (k_max − k_min)/m_0, j = 0, ..., m_0};  // Initialize knots
  // Main loop for enclosing an unknown number of zeros in intervals
  repeat {
    Compute φ'(κ), φ''(κ) for all κ ∈ S unlessdone already ;
    // Check for zeros of φ' close to elements of S ("knots")
    M := max_{ξ∈S} |φ'(ξ)| ;
    // Isolate knots where φ' is close to zero
    V := {i ∈ {0, ..., ♯S − 1} : |φ'(κ_i)| < τ_z M, [i − 1, i].isActive ∧ [i, i + 1].isActive} ;
    // Remove these knots and replace them with enclosing intervals
    foreach k ∈ V {
      S := S ∪ {κ_k − min{0.4τ_abs, ½(κ_k − κ_{k−1}), κ_k + min{0.4τ_abs, ½(κ_{k+1} − κ_k)} \ {κ_k} ;
      Set new intervals as 'Active' ;
    }
    seq<real> I := ∅ ;  // New knots to be inserted
    // Process all active intervals
    foreach i ∈ {1, ..., ♯S − 1}, [i − 1, i].isActive {
      α := κ_{i−1} ;  β := κ_i ;  // Current interval = [α, β]
      // φ' changes sign in the current interval
      if (φ'(α)φ'(β) ≤ 0) then {
        // Detect jump
        if (|φ'(α) − φ'(β)| / |β − α| > Γ · max{φ''(α), φ''(β)}) then
          { [i − 1, i].setNoZero; continue; }
        // Termination of recursion: zero found
        if (|α − β| ≤ τ_rel · min{|α|, |β|}) or (|α − β| ≤ τ_abs) then
          { [i − 1, i].setZero; continue; }
      }
      // Tentative cubic Hermite interpolation
      p ∈ P_3 : p(α) = φ'(α), p(β) = φ'(β), p'(α) = φ''(α), p'(β) = φ''(β) ;
      N := {ν_1 < ν_2 < ··· < ν_k} := {ν ∈ [α, β] : p(ν) = 0} ;
      // Add zeros of surrogate interpolating Hermite polynomial as knots
      if (N ≠ ∅) then I := I ∪ N ;
      else {
        μ := argmin{|p(ξ)|, ξ ∈ [α, β]} ;
        // If p comes close to zero there might be a zero of φ' in [α, β]
        if (|p(μ)| ≤ η min{|p(α)|, |p(β)|}) then I := I ∪ {μ} ;
        // Large intervals will always be split
        else if (|β − α| ≥ γ_split |b − a|) then I := I ∪ {½(α + β)} ;
        // Probably no zero in current active interval
        else [i − 1, i].setNoZero ;
    } }
    S := S ∪ I ;
    Set all new intervals 'Active' ;
  }
  until there are no active intervals left ;
  return midpoints of intervals marked as containing a zero ;
}
```

The second derivative of $k \mapsto \lambda(k)$ can be obtained by another differentiation of (35):

$$\lambda''(k) = 2\,\mathrm{Re}\{\mathbf{u}(k)^H \mathbf{W}'(k)\mathbf{u}'(k)\} + \mathbf{u}(k)^H \mathbf{W}''(k)\mathbf{u}(k)\ . \tag{38}$$

Here we made use of $\mathbf{W}'(k)^H = \mathbf{W}'(k)$ and that $\mathbf{u}'(k)$ is available from (37).

If $\lambda(k)$ is the smallest positive eigenvalue of $\mathbf{W}(k)$, then $\lambda(k) = \varphi(k)$. Therefore the computation of $\varphi'(k)$ and $\varphi''(k)$ entails finding the smallest positive eigenvalue of $\mathbf{W}(k)$ and an associated eigenvector, the solution of the linear system of equations (37), and the evaluation of (36) and (38).

*Remark* 7 (Computing $\mathbf{W}'(k)$ and $\mathbf{W}''(k)$). The Wieland matrix is built from boundary-element Galerkin matrices $\mathbf{A}(k)$ and $\mathbf{M}$ as has been explained in Section 3. The derivatives $\mathbf{A}'(k)$ and $\mathbf{A}''(k)$ can be computed as the boundary-element Galerkin matrices for boundary integral operators obtained by differentiating the kernels of the boundary integral operators from (7) with respect to $k$. This boils down to differentiating the fundamental solutions (6), which are analytic functions in $k$. Obviously, by the chain rule, differentiation with respect to $k$ will partly cancel the singularity of the integral kernels. This facilitates implementation.

*Remark* 8 (Detecting crossings). Above we have made the assumption that $\lambda(k)$ is a simple eigenvalue. In actual computations iterative eigensolvers will always compute a few of the smallest (in modulus) eigenvalues of $\mathbf{W}(k)$.

In the case of $\lambda(k)$ being a multiple eigenvalue the construction of a first order corrections for the eigenvalue expansion leads to the solution of Sylvester Matrix Equations which yield corrections of block Rayleigh Quotients instead of the simple Rayleigh Quotient from (36). In a sense a cluster of two very close eigenvalues is a perturbation of a single double eigenvalue, and so the introduction of the matrix equations techniques. For more information on the computational details of the analytic perturbation theory of multiple eigenvalues see [34, Section 2.5, and in particular Thm. 2.5.3.] for the expansion of block Rayleigh Quotient; see also [16] for comments on multiple eigenvalues and [2] for a practical algorithm. Given the fact that we have a perturbed problem – due to the projection process – we have opted to use the simple correction formulae and interpret them as being applied on a nearby problem with (within the perturbation tolerance) simple eigenvalues. The effect that the clustering of eigenvalues would have is in reducing the convergence radius of our expansion, but it would – at least locally – not make the expansion invalid.

## 6. Numerical Tests

We test our algorithm for the detection of local minima of $k \mapsto \varphi(k)$, that is, task **(TM)**, in two two-dimensional settings

(I) the unit disk $\Omega_i = \{\boldsymbol{x} \in \mathbb{R}^2 : \|\boldsymbol{x}\| < 1\}$, $n_i = 20$,
(II) the unit square $\Omega_i = ]0,1[^2$, $n_i = 20$.

In both cases the boundary element Galerkin discretization as detailed in Section 3 was based on partitions of $\Gamma := \partial\Omega_i$ into $N \in \mathbb{N}$ congruent panels.

| Parameter | $m_0$ | $\tau_z$ | $\tau_{\mathrm{abs}}$ | $\Gamma$ | $\tau_{\mathrm{rel}}$ | $\eta$ | $\Gamma_{\mathrm{split}}$ |
|---|---|---|---|---|---|---|---|
| Line in Listing 1 | 2 | 9 | 12 | 22 | 25 | 36 | 38 |
| Value | 3, 10 | $10^{-6}$ | $10^{-4}$ | 40 | $10^{-3}$ | 0.1 | 0.1 |

Table 1. Parameters for function `findZeros()` from Listing 1 used in the numerical experiments

Also in both cases we searched the minima in the range $k \in ]0,10[$. For the root finding algorithm of Listing 1 we used the parameters listed in Table 1. Of course, these values were tuned to give

good and reliable performance for both settings. There is no guarantee that they represent a good choice in other situations. Yet, we believe that the two test cases are sufficiently different to render a joint viable parameter set a reasonable choice for a wider range of cases.

6.1. **Impact of termination control parameter for Arnoldi method.** We use Arnoldi's method as implemented in Version 1.2 of the Arpack++ library[3] [15] to solve the linear eigenvalue problem encountered in the evaluation of $\varphi'(k)$ and $\varphi''(k)$, see Section 5.2. Specifically the reverse communication class for complex standard eigenvalue problems `ARrcCompStdEig` is used which provides an interface for using the `cnaupd` routine of Arpack which implements the implicitly restarted Arnoldi inverse iterations for the general complex eigenvalue problem. The necessary matrix vector products are computed using an LU decomposition provided by version 3.3.4 of Eigen. In Fig. 4 we display the impact of different values of the termination control parameter `tol` of the Arnoldi method [15, p. 79] on the detected minima. That parameter specifies a threshold for the relative accuracy of Ritz values, but its impact on the final accuracy of the computed eigenvalues remains obscure. We found that for `tol` $\leq 10^{-4}$ the termination error of Arnoldi's method did not affect the outcome of the root search any more: Then the dots in Fig. 4 are almost exactly on top of each other for different values of `tol` $\leq 10^{-4}$.

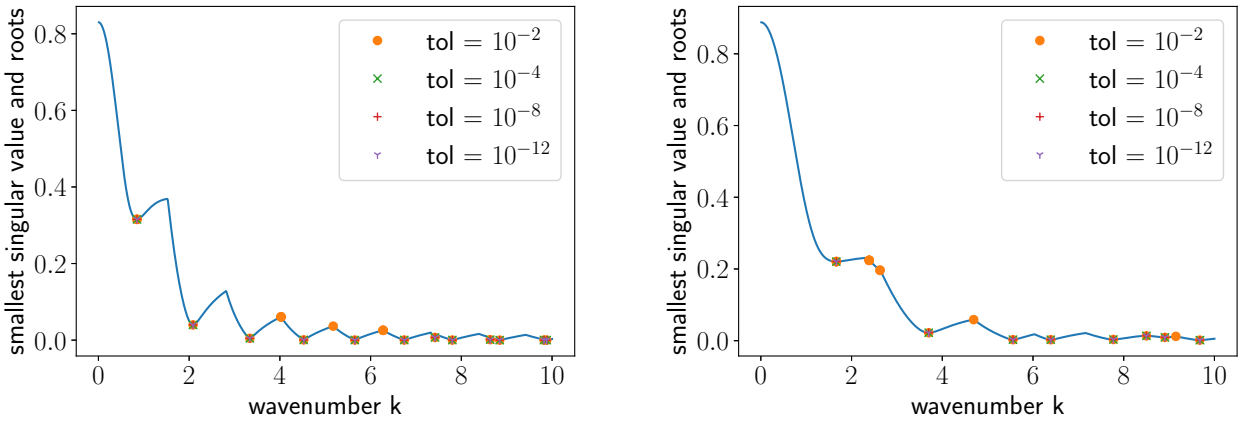


Unit disk, $N = 50$ Unit square, $N = 48$

FIGURE 4. Function $k \mapsto \varphi(k)$ and detected minima for different values of the termination control parameter `tol` of the implicitly restarted inverse Arnoldi method as accessed through the class `ARrcCompStdEig` of Arpack++, $m_0 = 10$.

6.2. **Empiric behavior of root finding for $\varphi'$.** For the two settings and $N = 50$, $N = 48$, respectively, we monitored the progress of the root finding algorithm `findZeros()` by tracking the evolution of the partition set $\mathcal{S}$ in the outer loop spanning Lines 4-44 of Listing 1. The results are visualized in Fig. 5 for Arnoldi termination control parameter equal to $10^{-4}$.

[3] `https://github.com/m-reuter/arpackpp`, last accessed March 2021

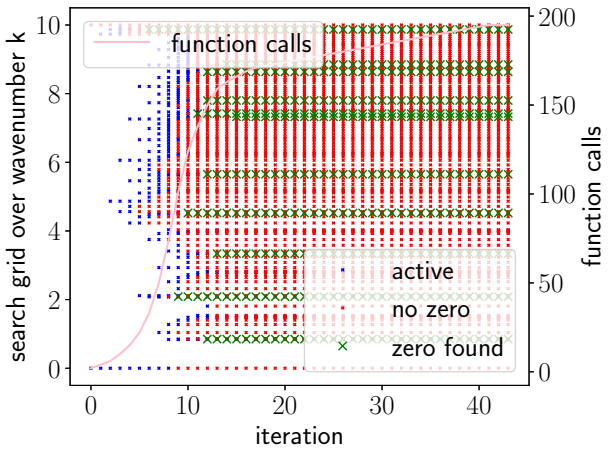


Unit disk, $m_0 = 1$

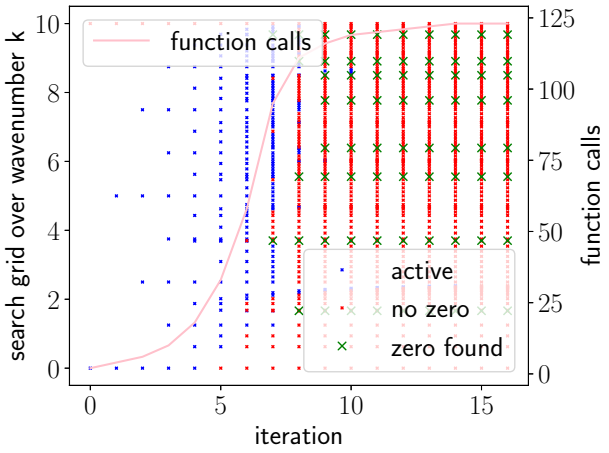


Unit square, $m_0 = 1$

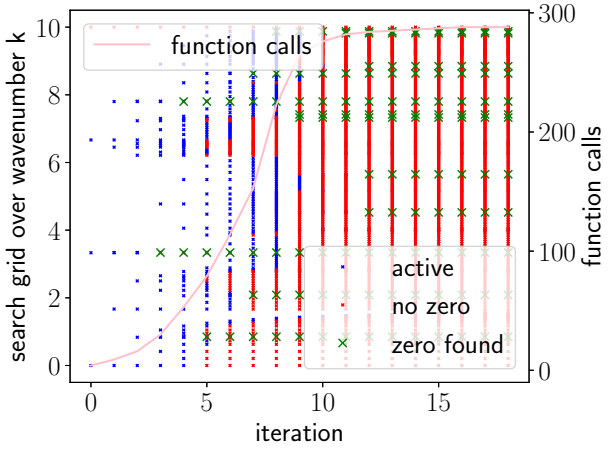


Unit disk, $m_0 = 3$

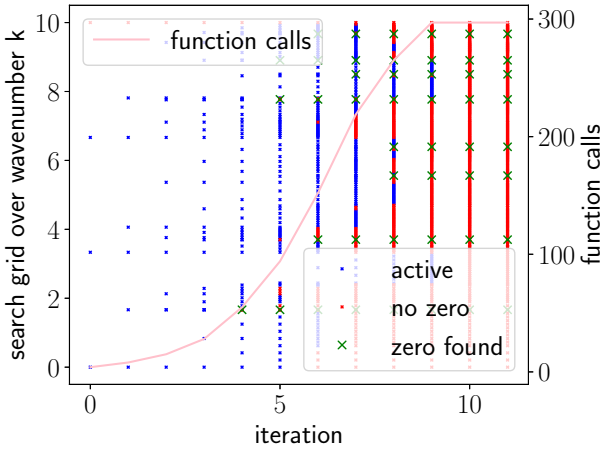


Unit square, $m_0 = 3$

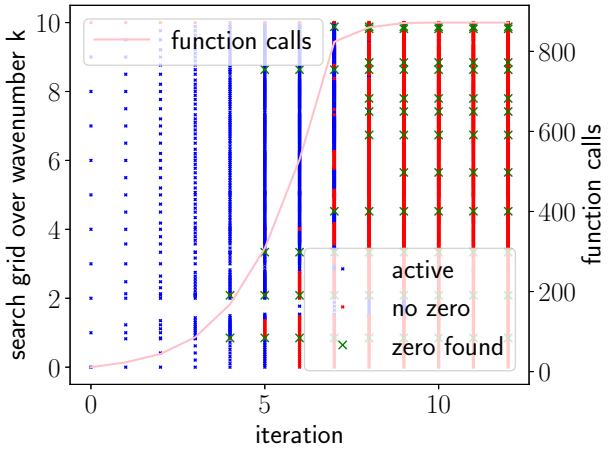


Unit disk, $m_0 = 10$

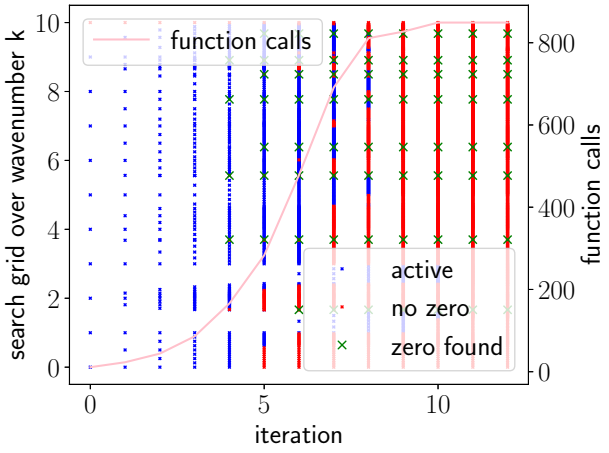


Unit square, $m_0 = 10$

FIGURE 5. Progress of iterative search for roots of $\varphi'$ for $m_0 = 10$. Blue sections of the $k$-interval may still contain zeros (Active intervals), while red sections are NoZero regions as discussed in Section 5.1. We also plot the cumulative number of evaluations of $(\varphi'(k), \varphi''(k))$ as required in Line 5 of Listing 1 (legend "function calls").

6.3. **Robustness and convergence of detected minima.** In another test we examined how the resolution of the boundary element discretization and the choice of the parameter $m_0$ (resolution of the initial partition for `findZeros()`, see Line 2, Listing 1) affect the detected zeros of $\varphi'$ in the two test cases. The red crosses in Fig. 6 and Fig. 7 show the found zeros for different numbers of panels and different numbers $m_0$ of initial search intervals. The numbers denoted by $\sharp\varphi -$ evals report the average number of the evaluations of $\varphi'(\kappa)$, and $\varphi''(\kappa)$ in Listing 1, Line 5. The termination control parameter `tol` for Arnoldi's method was set to $10^{-4}$.

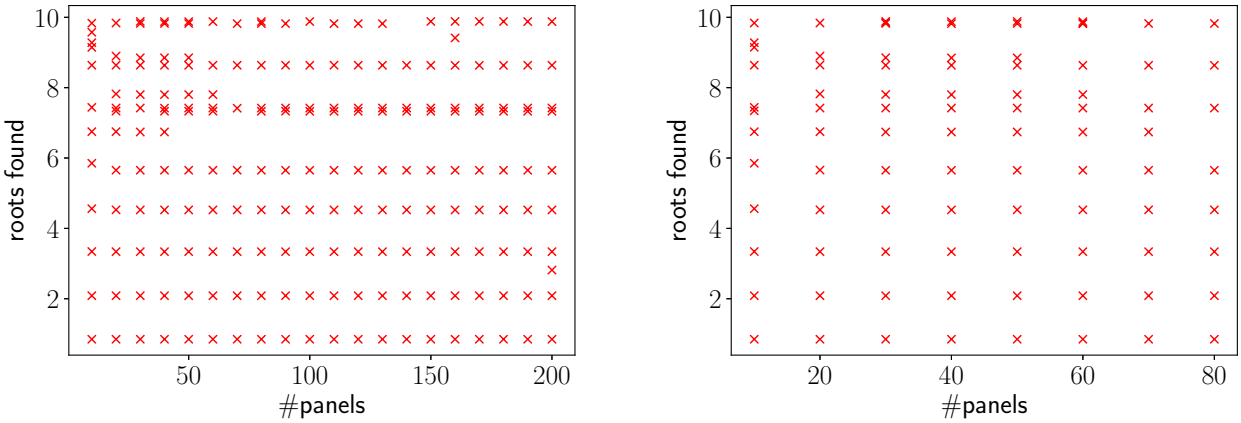


$m_0 = 3$, $\sharp\varphi -$ evals $= 297$ $m_0 = 10$, $\sharp\varphi -$ evals $= 880$

FIGURE 6. Numerical experiment of Section 6.3: unit disk

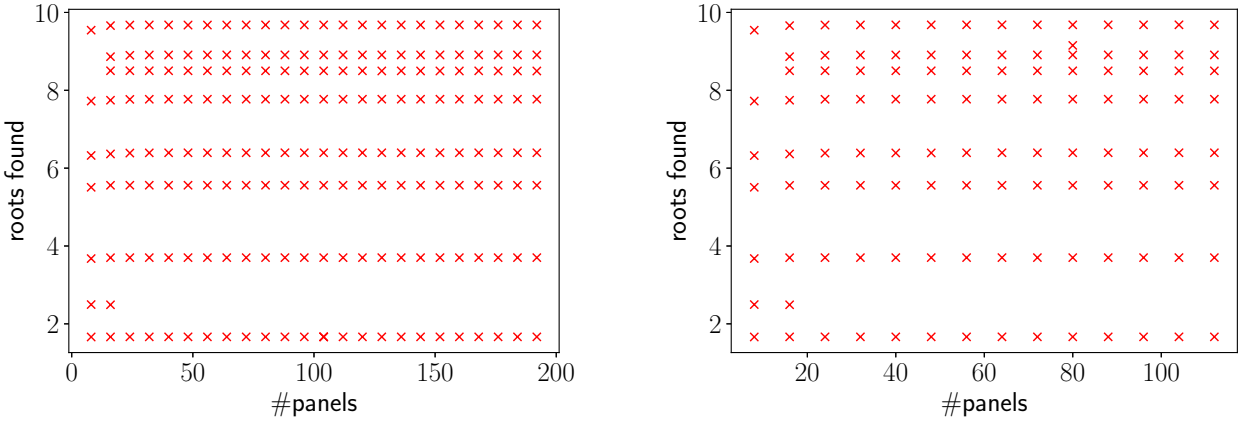


$m_0 = 3$, $\sharp\varphi -$ evals $= 307$ $m_0 = 10$, $\sharp\varphi -$ evals $= 863$

FIGURE 7. Numerical experiment of Section 6.3: unit square

The result of `findZeros()` depends on the discretization, but also on the initial subdivision of the $k$-interval. The former is not surprising for coarse meshes, nor is the latter in the presence of essentially flat sections of the graph of $\varphi$, where minima can easily escape detection. Fortunately, pronounced minima are found reliably and their location hardly depends on the mesh resolution.

## References


[1] S. Amini and N. D. Maines. "Preconditioned Krylov subspace methods for boundary element solution of the Helmholtz equation". In: *Internat. J. Numer. Methods Engrg.* 41.5 (1998), pp. 875–898. ISSN: 0029-5981. URL: https://doi.org/10.1002/(SICI)1097-0207(19980315)41:5%3C875::AID-NME313%3E3.0.CO;2-9.

[2] A. L. Andrew and R. C. E. Tan. "Computation of Derivatives of Repeated Eigenvalues and the Corresponding Eigenvectors of Symmetric Matrix Pencils". In: *SIAM Journal on Matrix Analysis and Applications* 20.1 (1998), pp. 78–100. eprint: https://doi.org/10.1137/S0895479896304332. URL: https://doi.org/10.1137/S0895479896304332.

[3] J. Asakura et al. "A numerical method for nonlinear eigenvalue problems using contour integrals". In: *JSIAM Lett.* 1 (2009), pp. 52–55. ISSN: 1883-0609. URL: https://doi.org/10.14495/jsiaml.1.52.

[4] V. Babich and V. Buldyrev. *Short-Wavelength Diffraction Theory. Asymptotic Methods*. Vol. 4. Springer Series on Wave Phenomena. Berlin: Springer, 1991.

[5] I. Babuška and J. Osborn. "Eigenvalue problems". In: *Handbook of numerical analysis, Vol. II*. Handb. Numer. Anal., II. North-Holland, Amsterdam, 1991, pp. 641–787.

[6] S. Balac, M. Dauge, and Z. Moitier. "Asymptotics for 2D whispering gallery modes in optical micro-disks with radially varying index". In: *IMA Journal of Applied Mathematics* 86.6 (Aug. 2021), pp. 1212–1265. URL: https://doi.org/10.1093%2Fimamat%2Fhxab033.

[7] S. Balac et al. "Mathematical analysis of whispering gallery modes in graded index optical micro-disk resonators". In: *The European Physical Journal D* 74.11 (Nov. 2020), p. 221. ISSN: 1434-6079. URL: https://doi.org/10.1140/epjd/e2020-10303-5.

[8] W.-J. Beyn. "An integral method for solving nonlinear eigenvalue problems". In: *Linear Algebra Appl.* 436.10 (2012), pp. 3839–3863. ISSN: 0024-3795. URL: http://dx.doi.org/10.1016/j.laa.2011.03.030.

[9] A. Bunse-Gerstner et al. "Numerical computation of an analytic singular value decomposition of a matrix valued function". In: *Numerische Mathematik* 60.1 (Dec. 1991), pp. 1–39. ISSN: 0945-3245. URL: https://doi.org/10.1007/BF01385712.

[10] T. Chaumont Frelet. "Finite element approximation of Helmholtz problems with application to seismic wave propagation". Theses. INSA de Rouen, Dec. 2015. URL: https://tel.archives-ouvertes.fr/tel-01246244.

[11] X. Claeys, R. Hiptmair, and C. Jerez-Hanckes. "Multi-trace boundary integral equations". In: *Direct and Inverse Problems in Wave Propagation and Applications*. Ed. by I. Graham et al. Vol. 14. Radon Series on Computational and Applied Mathematics. Berlin/Boston: De Gruyter, 2013, pp. 51–100.

[12] X. Claeys, R. Hiptmair, and E. Spindler. "A second-kind Galerkin boundary element method for scattering at composite objects". English. In: *BIT Numerical Mathematics* 55.1 (2015), pp. 33–57. ISSN: 0006-3835. URL: http://dx.doi.org/10.1007/s10543-014-0496-y.

[13] D. Colton and R. Kress. *Inverse Acoustic and Electromagnetic Scattering Theory*. 2nd. Vol. 93. Applied Mathematical Sciences. Heidelberg: Springer, 2013.

[14] B. Gavin, A. Miedlar, and E. Polizzi. "FEAST eigensolver for nonlinear eigenvalue problems". In: *J. Comput. Sci.* 27 (2018), pp. 107–117. ISSN: 1877-7503. URL: https://doi.org/10.1016/j.jocs.2018.05.006.

[15] F. M. GOMES and D. C. SORENSEN. *ARPACK++ - An object-oriented version of ARPACK eigenvalue package*. 1998. URL: https://github.com/m-reuter/arpackpp/blob/master/doc/arpackpp.pdf.

[16] A. Greenbaum, R.-C. Li, and M. L. Overton. "First-Order Perturbation Theory for Eigenvalues and Eigenvectors". In: *SIAM Review* 62.2 (2020), pp. 463–482.

[17] P. Heider. "Computation of scattering resonances for dielectric resonators". In: *Comput. Math. Appl.* 60.6 (2010), pp. 1620–1632. ISSN: 0898-1221. URL: http://dx.doi.org/10.1016/j.camwa.2010.06.044.

[18] H. Heuser. *Funktionalanalysis*. 2nd ed. Teubner–Verlag, Stuttgart, 1986.

[19] R. Hiptmair and C. Jerez-Hanckes. "Multiple traces boundary integral formulation for Helmholtz transmission problems". In: *Adv. Comput. Math.* 37.1 (2012), pp. 39–91. ISSN: 1019-7168. URL: http://dx.doi.org/10.1007/s10444-011-9194-3.

[20] R. Hiptmair, A. Moiola, and E. A. Spence. *Spurious Quasi-Resonances in Boundary Integral Equations for the Helmholtz Transmission Problem*. Tech. rep. 2021-28. https://arxiv.org/abs/2109.08530 Switzerland: Seminar for Applied Mathematics, ETH Zürich, 2021. URL: https://www.sam.math.ethz.ch/sam_reports/reports_final/reports2021/2021-28.pdf.

[21] R. Huang et al. "Recursive integral method for transmission eigenvalues". In: *J. Comput. Phys.* 327 (2016), pp. 830–840. ISSN: 0021-9991. URL: https://doi.org/10.1016/j.jcp.2016.10.001.

[22] R. Kress. *Linear Integral Equations*. Vol. 82. Applied Mathematical Sciences. Berlin: Springer, 1989.

[23] P. Lietaert et al. "Automatic rational approximation and linearization of nonlinear eigenvalue problems". In: *IMA J. Numer. Anal.* 42.2 (2022), pp. 1087–1115. ISSN: 0272-4979. URL: https://doi.org/10.1093/imanum/draa098.

[24] J. Mäkitalo, M. Kauranen, and S. Suuriniemi. "Modes and resonances of plasmonic scatterers". In: *Phys. Rev. B* 89 (16 Apr. 2014), p. 165429. URL: http://link.aps.org/doi/10.1103/PhysRevB.89.165429.

[25] W. McLean. *Strongly Elliptic Systems and Boundary Integral Equations*. Cambridge, UK: Cambridge University Press, 2000. ISBN: 0-521-66332-6/hbk, 0-521-66375-X/pbk.

[26] R. Misawa, K. Niino, and N. Nishimura. "Boundary integral equations for calculating complex eigenvalues of transmission problems". In: *SIAM J. Appl. Math.* 77.2 (2017), pp. 770–788. ISSN: 0036-1399. URL: https://doi.org/10.1137/16M1087436.

[27] A. Moiola and E. A. Spence. "Acoustic transmission problems: wavenumber-explicit bounds and resonance-free regions". In: *Math. Models Methods Appl. Sci.* 29.2 (2019), pp. 317–354. ISSN: 0218-2025. URL: https://doi.org/10.1142/S0218202519500106.

[28] J. E. Osborn. "Spectral approximation for compact operators". In: *Math. Comput.* 29 (1975), pp. 712–725. ISSN: 0378-4754.

[29] B. N. Parlett. *The symmetric eigenvalue problem*. Vol. 20. Classics in Applied Mathematics. Corrected reprint of the 1980 original. Society for Industrial and Applied Mathematics (SIAM), Philadelphia, PA, 1998, pp. xxiv+398. ISBN: 0-89871-402-8. URL: http://dx.doi.org/10.1137/1.9781611971163.

[30] G. Popov and G. Vodev. "Resonances near the real axis for transparent obstacles". In: *Comm. Math. Phys.* 207.2 (1999), pp. 411–438. ISSN: 0010-3616. URL: https://doi.org/10.1007/s002200050731.

[31] D. Pradovera. "Interpolatory rational model order reduction of parametric problems lacking uniform inf-sup stability". In: *SIAM J. Numer. Anal.* 58.4 (2020), pp. 2265–2293. ISSN: 0036-1429. URL: https://doi.org/10.1137/19M1269695.

[32] S. Sauter and C. Schwab. *Boundary Element Methods*. Vol. 39. Springer Series in Computational Mathematics. Heidelberg: Springer, 2010.

[33] P. Stefanov. "Quasimodes and resonances: Sharp lower bounds". In: *Duke Mathematical Journal* 99.1 (1999), pp. 75–92. URL: https://doi.org/10.1215/S0012-7094-99-09903-9.

[34] J.-G. Sun. *Stability and accuracy: Perturbation analysis of algebraic eigenproblems*. Technical Report UMINF 98.07. Umeå University, Department of Computer Science, 1998. URL: https://people.cs.umu.se/jisun/Jiguang-Sun-UMINF98-07-rev2002-02-20.pdf.

[35] S.-H. Tang and M. Zworski. "From quasimodes to resonances". In: *Mathematical Research Letters* 5 (1998), pp. 261–272.

[36] R. H. Torres and G. V. Welland. "The Helmholtz equation and transmission problems with Lipschitz interfaces". In: *Indiana Univ. Math. J.* 42.4 (1993), pp. 1457–1485. ISSN: 0022-2518. URL: http://dx.doi.org/10.1512/iumj.1993.42.42067.

[37] D. Werner. *Funktionalanalysis*. Berlin: Springer, 1995.

[38] J. Xiao et al. "Solving large-scale nonlinear eigenvalue problems by rational interpolation and resolvent sampling based Rayleigh-Ritz method". In: *Internat. J. Numer. Methods Engrg.* 110.8 (2017), pp. 776–800. ISSN: 0029-5981. URL: https://doi.org/10.1002/nme.5441.

[39] S. Yokota and T. Sakurai. "A projection method for nonlinear eigenvalue problems using contour integrals". In: *JSIAM Lett.* 5 (2013), pp. 41–44. ISSN: 1883-0609. URL: https://doi.org/10.14495/jsiaml.5.41.